*Published online 15 December 2015*

*Nucleic Acids Research, 2016, Vol. 44, No. 2* ***983–991***
*doi: 10.1093/nar/gkv1384*

# Different duplex/quadruplex junctions determine the properties of anti-thrombin aptamers with mixed folding

**Irene Russo Krauss[1,2], Vera Spiridonova[3], Andrea Pica[1,2], Valeria Napolitano[1] and Filomena Sica[1,2,*]**

[1]Department of Chemical Sciences, University of Naples 'Federico II', Naples, Italy, [2]Institute of Biostructures and Bioimages, C.N.R, Naples, Italy. and [3]A.N. Belozersky Institute of Physico-Chemical Biology, M.V. Lomonosov Moscow State University, 119992 Moscow, Russia

Received November 03, 2015; Revised November 25, 2015; Accepted November 26, 2015



## ABSTRACT

**Mixed duplex/quadruplex oligonucleotides have attracted great interest as therapeutic targets as well as effective biomedical aptamers. In the case of thrombin-binding aptamer (TBA), the addition of a duplex motif to the G-quadruplex module improves the aptamer resistance to biodegradation and the affinity for thrombin. In particular, the mixed oligonucleotide RE31 is significantly more effective than TBA in anticoagulation experiments and shows a slower disappearance rate in human plasma and blood. In the crystal structure of the complex with thrombin, RE31 adopts an elongated structure in which the duplex and quadruplex regions are perfectly stacked on top of each other, firmly connected by a well-structured junction. The lock-and-key shape complementarity between the TT loops of the G-quadruplex and the protein exosite I gives rise to the basic interaction that stabilizes the complex. However, our data suggest that the duplex motif may have an active role in determining the greater anti-thrombin activity in biological fluids with respect to TBA. This work gives new information on mixed oligonucleotides and highlights the importance of structural data on duplex/quadruplex junctions, which appear to be varied, unpredictable, and fundamental in determining the aptamer functional properties.**

## INTRODUCTION

DNA structures, different from the canonical B-form double helix, have been known for a long time and extensively characterized. Several studies have also highlighted the remarkable shape variability of nucleic acids (1) and its close connection to the specific functions of these molecules. The alternative folds include various kind of double helices (2), triplex arrangements (3), four way Holliday junctions (4), i-motifs (5), and G-quadruplexes (6). The latter are particularly interesting because have been found in telomeric ends of chromosomes (7), in oncogenes (8) and in the promoter regions (9).

G-quadruplexes are formed by stacked G-tetrads, which are cyclic arrays of four guanines interacting through Hoogsteen hydrogen bonds. Depending on strand directionality, glycosidic bond angles, loop length and conformation, different G-quadruplex topologies have been observed (6).

Thanks to the numerous crystallographic (10) and NMR (11) structures of G-quadruplexes determined in the last decades, our knowledge of these peculiar motifs is considerably grown. Thus, in the last years the interest has moved towards the way these structures interface with other structural motifs (12), such as other quadruplexes (13–15) or duplexes (12,16,17). In particular, an intriguing issue concerns the way duplexes and quadruplexes, which are often characterized by different strand directionality, groove width and base orientation, can found accommodation in the same molecule. Recently, Phan *et al.* (17,18) have shown, through the NMR characterization of artificial constructs, several modes in which quadruplexes and duplexes can be connected (17). However, the molecules they investigated were designed to adopt a specific fold through the insertion of strand breakers or additional residues in key regions to promote the quadruplex–duplex transition. Much less is known about the fold of oligonucleotides in which these specific markers are not present. This is of particular interest in the case of aptamers, DNA (19) and RNA (20) strands able to bind with very high affinity and selectivity a large variety of molecules, ranging from small molecules, other oligonucleotides, peptides or large proteins (21). This ability mainly depends on the aptamer propensity to fold into several distinct three-dimensional shapes, which are difficult to establish *a priori*. Indeed, aptamers

*To whom correspondence should be addressed. Tel: +39 081 674479; Fax: +39 081 674090; Email: filosica@unina.it

against a specific target are usually selected from random libraries of about $10^{10}$–$10^{20}$ sequences by SELEX (21). Using this procedure, aptamers against many pathologically relevant proteins (22), such as thrombin, nucleolin, HIV RNase H, prion and many others, have been selected (23–26). The variety of folds these oligonucleotides may adopt includes also a duplex/quadruplex mixed structure. Based on their sequence, this very peculiar structure has been suggested to be adopted by an anti-RANK (human receptor activator of NF-kB) aptamer, the aptamer against the HIV RNaseH and several anti-thrombin aptamers (23), such as HD22 and RE31. HD22 aptamers (24) include a 27- and a 29-mer able to bind the exosite II of thrombin with an affinity about 100–200 times higher than that of the best known thrombin binding aptamer TBA, which recognizes exosite I (19). The 31-mer RE31 (25) is a new generation aptamer with increased affinity towards exosite I (26,27) and improved performances in biological fluids (28) with respect to TBA. The latter has been shown (29–32) to adopt a unimolecular G-quadruplex structure that includes two G-tetrads, two TT loops and a TGT loop (Figure 1A). Moreover, X-ray diffraction analysis has clearly shown that the binding motif of this molecule involves the two TT loops (29–31). HD22 and RE31 were supposed to have a TBA-like G-quadruplex (Figure 1B and C) and a terminal duplex segment connected by two linkers three- and two-residue long for HD22 (24) and RE31 (26–28,32), respectively. The proposed global fold for the two aptamers is rather similar in contrast to their very different properties.

Some of us have recently solved the crystal structure of HD22 in complex with thrombin (33) demonstrating that it adopts a fold different from that previously proposed and depicted in Figure 1B. The structure embodies a duplex segment strictly connected to a highly distorted G-quadruplex (*pseudo*-quadruplex), in an unexpected perpendicular arrangement of the two regions. This peculiar steric combination favours the binding at the exosite II, with which both motifs interact (33).

Here, we present the crystal structure of the complex between thrombin and RE31, which clearly shows that the aptamer binds at the exosite I and adopts a markedly different fold with respect to HD22. The aptamer presents an elongated structure in which three base pairs mediate the transit from the duplex to the quadruplex region, determining a continuous base stacking that includes both regions. The results also provide a structural based interpretation of the improved binding and inhibitory properties of RE31 compared to TBA (26).

## MATERIALS AND METHODS

### Sample preparation and crystallization

The RE31 aptamer, namely 5′-GTGACGTAGGTT GGTGTGGTTGGGGCGTCAC-3′ was purchased from Syntol (Russia). The human D-Phe-Pro-Arg-chloromethylketone (PPACK)-inhibited thrombin was purchased from Haemtech (USA).

A stock solution of the aptamer was prepared at a concentration of about 1 mM in 100 mM potassium chloride, 10 mM potassium cacodylate pH 7.0. This solution was heated for 10 min at 85°C and then slowly cooled down and stored at 20°C overnight, in order to induce folding. The correct fold was verified by recording circular dichroic spectra in the 200–350 nm range. The complex with thrombin was prepared as previously described (29,30,34) by placing a 1.2-fold molar excess of aptamer on a frozen sample of inhibited thrombin and leaving the sample for 3 h at 4°C. Then, the sample was diluted and the buffer changed to 25 mM K-phosphate pH 7.1 and 100 mM KCl. The thrombin–RE31 complex was finally concentrated to about 7 mg/ml using 10 kDa-cutoff Centricon mini-concentrator and a refrigerated centrifuge.

Initial crystallization trials were set up using commercial kits and an automated crystallization workstation (Hamilton Robotics). In a couple of days, well-formed crystals grew in many different conditions. The best diffracting ones (Supplementary Figure S1) grew from drops consisting of 0.6 μl thrombin-RE31 solution and 0.6 μl reservoir solution (200 mM sodium malonate pH 7, 18% w/v PEG 3350 Da) that were equilibrated against 500 μl reservoir solution.

### Data collection, structure determination and refinement

Diffraction data were collected in-house on a Saturn944 CCD detector. The X-ray radiation used was Cu-Kα radiation from a Rigaku Micromax 007 HF generator. After the addition of 25% (v/v) glycerol to the harvesting solution, crystals were flash-cooled at 100 K in supercooled $N_2$ gas (Oxford Cryosystems) and maintained at 100 K during the data collection. Diffraction data were processed using HKL2000 (35). Crystals of thrombin-RE31 complex belong to the orthorhombic space group $P2_12_12$ and diffract up to 2.99 Å resolution. Matthews' coefficient calculations suggested the presence of a 1:1 complex in the asymmetric unit and a solvent content of 45%. Detailed statistics on data collection are reported in Supplementary Table S1.

The structure was solved using the program Phaser (36). The coordinates of thrombin and the two G-planes of TBA, which were derived from the structure of the thrombin-TBA complex (PDB code: 4DII) (30), were utilized as two independent search models. A clear solution was obtained with a *Z*-score of 14.3 and a log-likelihood gain (LLG) of 848.

The starting model was refined using Refmac5 (37) and Phenix (38) programs. Each run was alternated with manual model building using WinCoot (39). Analysis of electron density maps, calculated with ($F_o$ – $F_c$) and ($2F_o$ – $F_c$) coefficients, allowed the rebuilding of the aptamer missing residues, with the only exception of the two terminal 5′ and 3′ residues, the positioning of a potassium ion in the quadruplex core and of several water molecules.

The final model has R-factor/Rfree values of 0.166/0.231. Statistics and parameters of the refinement are given in Supplementary Table S2.

The drawings were prepared with Pymol (http://pymol.org) and Chimera (40). The coordinates of the structure have been deposited in the Protein Data Bank (Code 5CMX).

### Structural analysis

3DNA-dssr (41) was used to calculate local and overall geometric parameters of the aptamer. Superpose program

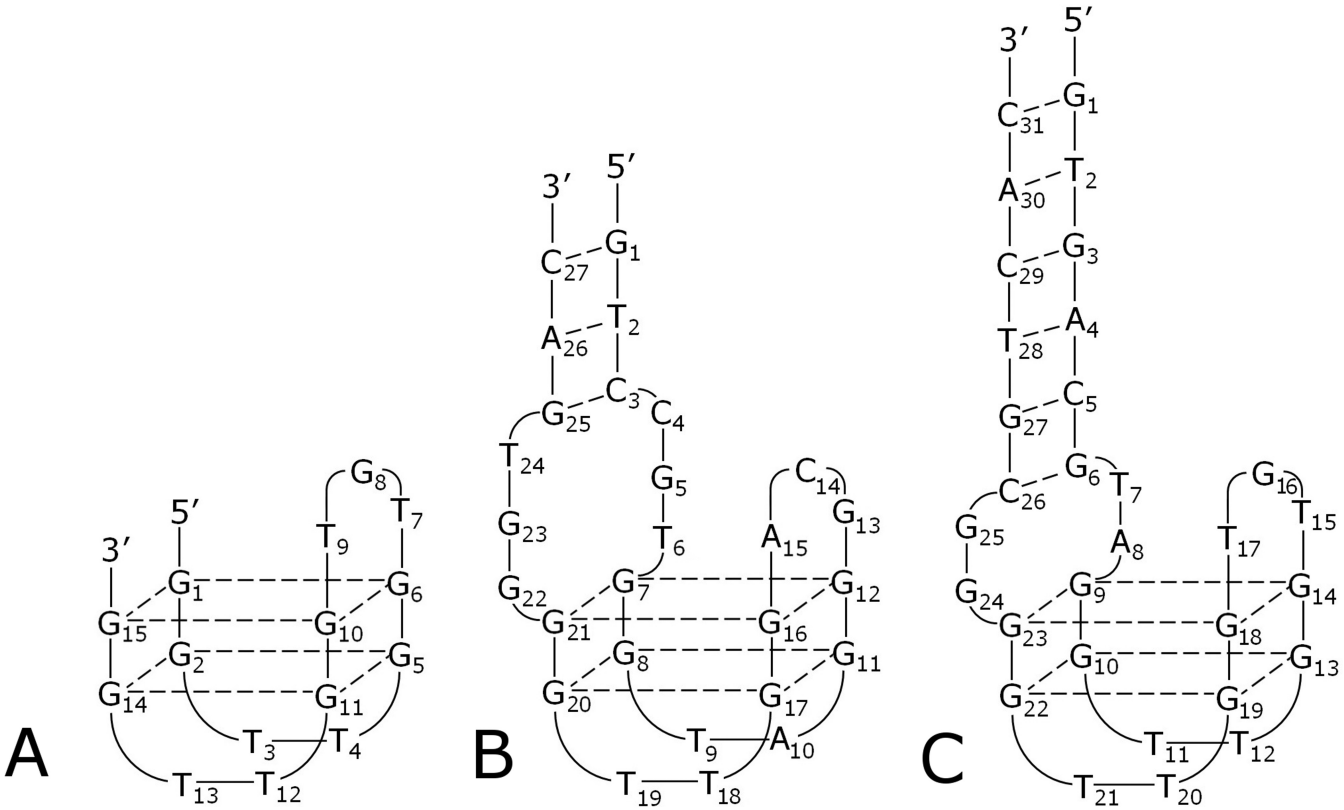


**Figure 1.** Schematic representation of the structure of TBA (**A**) and of the organization proposed on the basis of sequence for HD22–27mer (**B**) and RE31 (**C**).

from CCP4 package (42) was used to calculate root mean square deviations. Features of the thrombin–RE31 interface were calculated using Cocomaps server (43), whereas contacts between the two molecules, as well as packing interactions between the aptamer and symmetry related thrombin molecules, were found by using 3DNA-snap (41) and Pisa (44) programs. All the results were verified by visual inspection of the structure with WinCoot (39).

## RESULTS

### Overall crystal structure

Best crystals of the complex between thrombin and RE31 in the presence of $K^+$, diffract X-rays up to a resolution of 2.99 Å and belong to orthorhombic space group $P2_12_12$. Initial model obtained by molecular replacement showed that the aptamer G-planes are located close to thrombin exosite I. Electron density maps calculated from initial phases allowed unambiguous model building of the whole DNA molecule (Figure 2A and B), with the only exception of the terminal residues (Gua1 and Cyt31). For what concerns thrombin, the heavy chain (residues 16–245) and the light chain (residues 1B-14K) were well defined in the electron density maps, with the exception of the γ-autolysis loop (residues 146–150) of the heavy chain. The crystal structure was refined to Rfactor/Rfree values of 0.166/0.231, respectively. Detailed statistics of the refinement process are reported in Supplementary Table S2.

### Global aptamer fold

Based on sequence analysis and spectrophotometric studies in solution, a mixed duplex–quadruplex structure was proposed for RE31 aptamer (Figure 1C) (25,28,32); crystallographic analysis shows that RE31 in complex with thrombin indeed adopts this mixed fold.

Moreover, good quality electron density maps (Figure 2B) allowed a very detailed description of the aptamer fold. Five Watson–Crick base pairs, starting with the Thy2–Ade30 pair, define a regular B-type double helix. Two additional non-Watson–Crick base pairs formed by residues belonging to linkers and loops extend further the duplex region. The quadruplex motif involves the fifteen TBA-residues arranged in the well-known chair-like fold (30), with two G-tetrads (residues 10, 13, 19, 22 for tetrad I, and 9, 14, 18, 23 for tetrad II), which coordinate a potassium ion, two TT loops and a TGT loop. The latter is in close proximity to the duplex segment, and, in particular, is directly involved in the transition from the duplex to the quadruplex segment (see the following section). After superposition of the quadruplex core of RE31 and TBA, excluding the TGT loop, the root mean square deviation (RMSD) between all the atoms of the two G-quadruplexes is only 0.89 Å, indicating that the overall fold of the quadruplex remains basically unaltered. The quadruplex domain of RE31 keeps the alternating *syn-anti* conformation for each adjacent pair of guanines along the strand and the

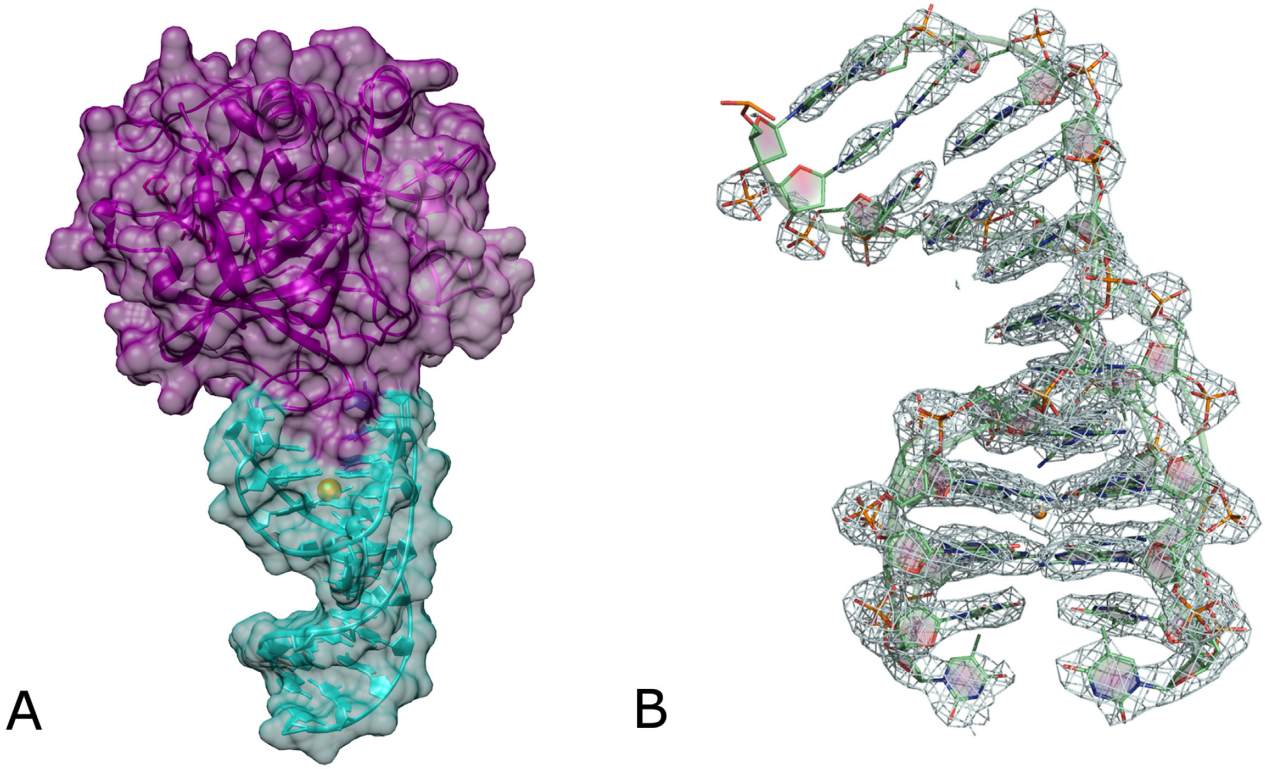


**Figure 2.** (**A**) Surface/cartoon representation of thrombin–RE31 complex. Thrombin heavy and light chain are coloured dark and light magenta, respectively, the aptamer is coloured cyan and the potassium ion orange. (**B**) $2F_o - F_c$ electron density maps of the RE31 aptamer contoured at 1.5$\sigma$ level.

cyclic array of Hoogsteen-like hydrogen bonds in each tetrad.

The two tetrads are essentially planar, with RMSD values calculated with respect to the average G-quartet planes of 0.37 and 0.42 Å for tetrads I and II, respectively, in very good agreement with values obtained for TBA (0.35 and 0.39 Å, for TBA in complex with thrombin in the presence of $K^+$ ions, PDB code 4DII). The similarity between TBA and the TBA-portion of RE31 extends to position of bases belonging to TT loops. Indeed, thymines 12 and 21 stack on the G-tetrad I and are connected to each other through a water molecule, similarly to the Thy4-Thy13 pair of TBA. Minimal differences are observed for Gua18, whose position is fixed by the stacking geometry of Thy17 and the other core guanines (see below).

Careful analysis of the duplex region (Supplementary Table S3) highlights the regularity of the structure, despite the presence of the quadruplex, likely due to the gradual transition from one motif to the other.

### Duplex/quadruplex junction

On the basis of the sequence, the duplex and the quadruplex motifs of RE31 were supposed (25,28,32) to be connected by two 2-residue linkers (TA and GG respectively) (Figure 1C). This suggestion is not validated by the crystal structure. Indeed the TGT loop from the quadruplex region is involved in the transition between the two domains by forming base pairs with residues from the linkers. Overall, three base pairs constitute the duplex/quadruplex junction (Figure 3). At the end of the double helix, the first two residues from the linkers (Thy7 and Gua25) form a Wobble pair. In the second pair (Ade8 and Thy17), the bases are linked through a reverse Hoogsteen hydrogen bond network. It is worth to stress that Thy17 is part of the TGT loop. The last loose pair presents a non-canonical G-G interaction between Gua24 and Gua16; the latter is the guanine of the TGT loop. Detailed hydrogen-bonded interactions among residues of the junction are reported in Table 1 and depicted in Supplementary Figure S2. It should be stressed that the first base pair, Thy7–Gua25 is planar and well integrated in the duplex segment; whereas the last one, Gua16–Gua24, barely defines a plane. However, the arrangement of these six residues is such that a continuous stacking from the duplex segment to the quadruplex one is observed (Table 2). In particular, Thy7, Thy17 and Gua16 (junction) are aligned with Gua6 (duplex) and Gua14 (quadruplex) and Gua25, Ade8 and Gua24 (junction) are aligned with Cyt26 (duplex) and Gua23 (quadruplex) (Figure 4). The junction pairs are also crucial to mediate the change of groove width from 17 Å (measured for the P–P distance) for the minor groove of the duplex to 19 Å for the wide groove of the quadruplex.

### Thrombin–RE31 interaction

In the asymmetric unit RE31 binds exosite I of thrombin through its quadruplex motif in a manner very similar to TBA (30). Detailed interactions between thrombin and RE31 are reported in Table 3. Comparing these data with those previously obtained for TBA (30), it is clear that

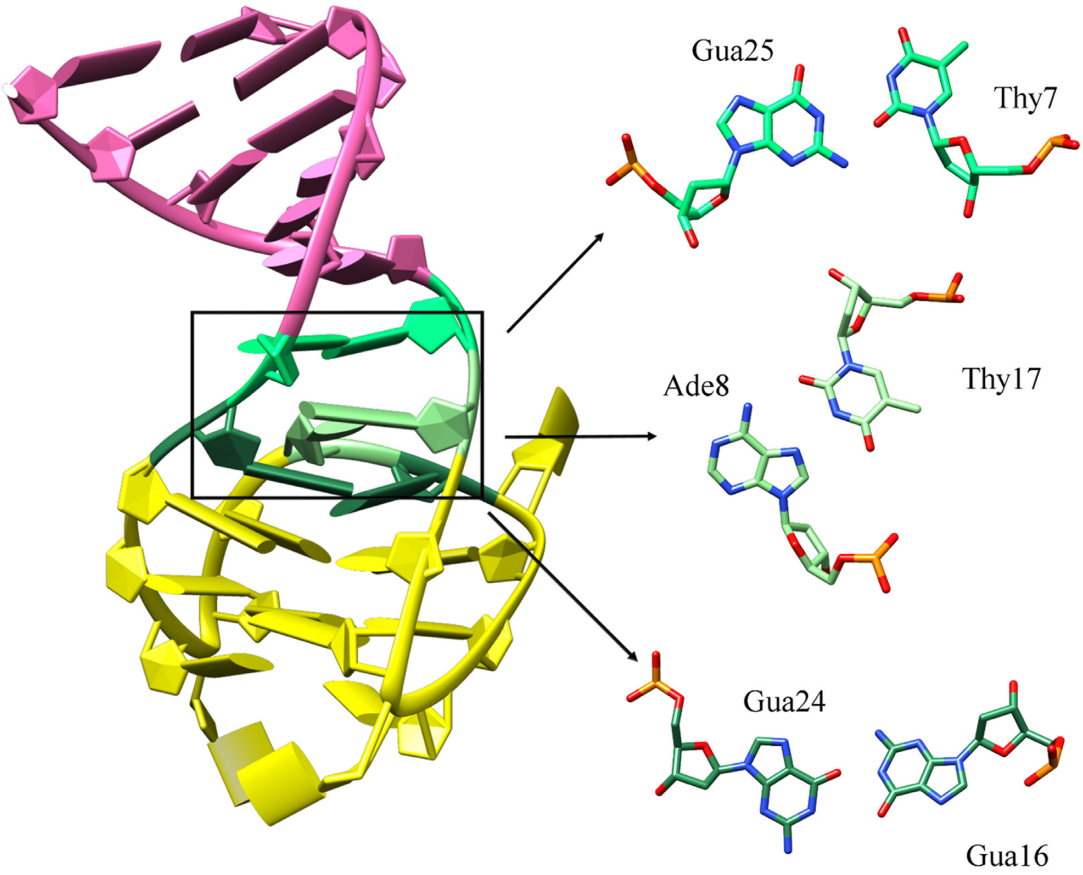


**Figure 3.** The duplex/quadruplex junction in RE31 aptamer. On the left a cartoon representation of the aptamer with different motifs marked in different colours (duplex segment in pink, quadruplex segment in yellow, the junction in green), on the right stick representation of the three base pairs composing the junction.

**Table 1.** Hydrogen-bonded interactions among residues of the duplex/quadruplex junction of RE31

| Atom | Nucleotide 1 | Atom | Nucleotide 2 | Distance (Å) |
|---|---|---|---|---|
| O2 | Thy7 | N2 | Gua25 | 2.6 |
| O2 | Thy7 | N1 | Gua25 | 2.7 |
| N7 | Ade8 | N3 | Thy17 | 2.5 |
| N7 | Ade8 | O4 | Thy17 | 2.3 |
| N6 | Ade8 | O2 | Thy17 | 2.9 |
| N2 | Gua16 | O6 | Gua24 | 2.8 |
| N1 | Gua16 | O6 | Gua24 | 2.6 |

the differences in the mode of binding of the two molecules are negligible, despite the doubled size of RE31. Hydrogen bonds, as well as hydrophobic interactions, with the target protein are very well conserved (Figure 5). It should be noted that none of the residues belonging to the duplex or the junction region of RE31 is involved in the stabilization of the binary complex.

## Crystal packing

In addition to the aptamer–thrombin interactions described above, the duplex segment of RE31 is in contact with three symmetry related thrombin molecules (Supplementary Figure S3). In particular, the phosphate group of Thy28 strongly interacts with two arginine side chains of the molecule at −x-1/2, y-1/2, −z-1: salt bridges are formed between OP1 and OP2 of Thy28 and guanidinium groups of Arg126 and Arg233, belonging to thrombin exosite II. Less strong interactions are found between RE31 and the thrombin molecule at −x-1/2, y-1/2, −z-2. In this case the protein caps the end of the duplex with residues Pro60B, Pro60C, Trp96 and Arg97 burying an interface area of 158 Å$^2$. Finally, Thy15, one of the three residues not involved in intramolecular contacts (the other two, Thy11 and Thy20, bind exosite I), occupies a patch on surface of the molecule at −x-1, −y, z, defined by residues Phe34,

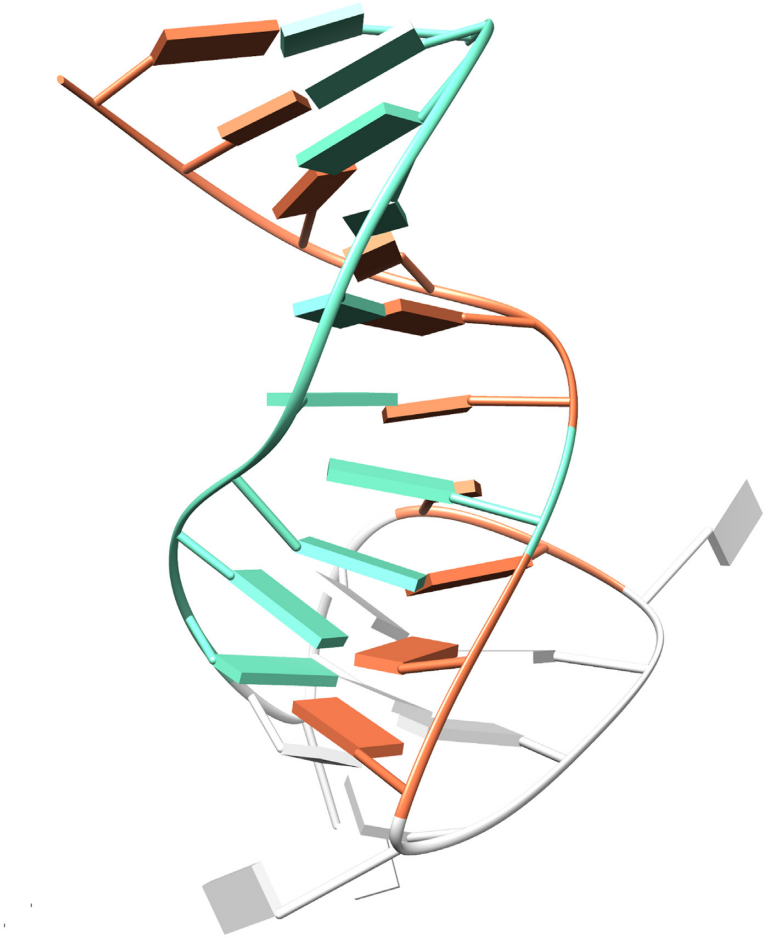

**Figure 4.** Ribbon representation of RE31 highlighting the continuous stacking of bases from the duplex to the quadruplex region.

**Table 2.** Stacking interactions as calculated by 3DNA-DSSR (41) among residues belonging to the duplex, the junction and the quadruplex of RE31

| Nucleotide 1 | Nucleotide 2 | Structural motif | Base stacking (Å$^2$)[a] |
|---|---|---|---|
| Ade2 | Cyt3 | Duplex | 5.7 |
| Cyt3 | Thy4 | Duplex | 7.2 |
| Thy4 | Gua5 | Duplex | 3.3 |
| Gua5 | Gua6 | Duplex | 4.8 |
| Gua6 | Thy7 | Junction | 6.7 |
| Thy7 | Thy17 | Junction | 6.0 |
| Thy17 | Gua16 | Junction | 8.9 |
| Gua16 | Gua14 | Junction | 2.7 |
| Gua14 | Gua13 | Quadruplex | 4.2 |
| Thy30 | Gua29 | Duplex | 4.1 |
| Gua29 | Ade28 | Duplex | 3.0 |
| Thy28 | Cyt27 | Duplex | 5.5 |
| Cyt27 | Cyt26 | Duplex | 2.4 |
| Cyt26 | Gua25 | Junction | 4.4 |
| Gua25 | Ade8 | Junction | 2.3 |
| Ade8 | Gua24 | Junction | 5.3 |
| Gua24 | Gua23 | Junction | 2.5 |
| Gua23 | Gua22 | Quadruplex | 3.8 |

[a]Base-stacking is quantified as the area of the overlapped polygon defined by the two bases of the interacting nucleotides, where the base atoms are projected onto the mean base plane.

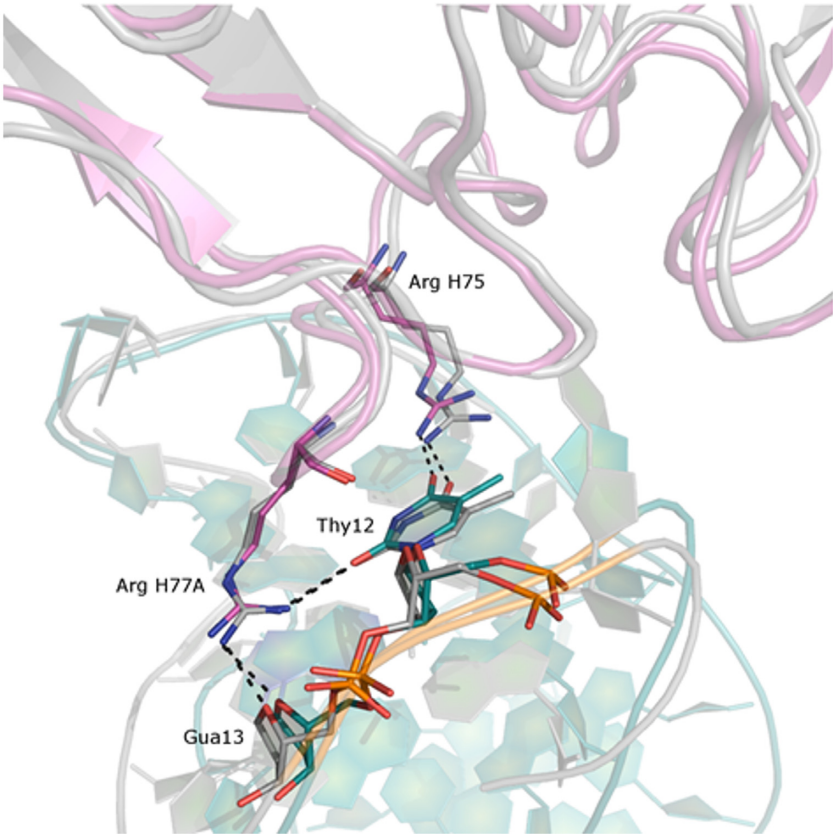


**Figure 5.** Comparison of interaction within thrombin–RE31 (protein molecule depicted in magenta and aptamer molecule in teal) and thrombin–TBA (colored in gray) complexes. Polar contacts between Arg H75, Arg H77A, Thy12 (Thy4 in TBA) and Gua13 (Gua5 in TBA) are highlighted.

**Table 3.** Interactions between thrombin and RE31

| | Hydrogen bonds | | | | Hydrophobic contacts |
|---|---|---|---|---|---|
| RE31 residue | Atom | Thrombin residue | Atom | Distance (Å) | Thrombin residue |
| Thy11 | O3' | Tyr117 | OH | 3.28 | Ile24, His71, Ile79, Tyr117 |
| | N3 | Glu77 | OE2 | 2.97 | |
| Thy12 | O4 | Arg75 | NH2 | 2.28 | Asn78, Ile79 |
| | O2 | Arg77A | NH1 | 2.76 | |
| Gua13 | O4' | Arg77A | NH2 | 2.87 | |
| | OP1 | Asn78 | ND2 | 3.49 | |
| Thy20 | | | | | Tyr76 |
| Thy21 | O2 | Arg75 | NE | 2.87 | Tyr76 |
| | O2 | Arg75 | NH2 | 3.28 | |
| | O4' | Tyr76 | N | 2.87 | |

Lys36, Gln38, Leu65, Arg67, Tyr76, Lys81, Ile82, Met84. Thy15 also contacts Thy20 of the corresponding aptamer. Although the interface areas of the duplex contacts are appreciable, they are much less extended than that relative to the well-characterized TT loops-exosite I interface (586.2 $Å^2$).

## DISCUSSION

The structural investigation on oligonucleotides able to adopt a mixed duplex/quadruplex fold is still understated, despite the great interest these molecules assume in different biological contexts, including the case of several biomedical aptamers (23).

The present crystallographic analysis shows that RE31 adopts a mixed duplex/quadruplex fold, as it was previously suggested using a combination of spectrophotometric studies in solution and sequence analogies with well characterized molecules such as the 15-mer TBA with which RE31 share the sequence of the core residues. Indeed, these fifteen residues adopt the antiparallel G-quadruplex structure observed for TBA (30). However, in RE31 the TGT loop is crucially involved in the transit from the duplex to the quadruplex region with the result that a continuous base stacking runs along the whole molecule: the duplex gradually converts into the quadruplex organization and the helical axes of the two regions maintain almost the same orientation. This rod-like shape prevents a simultaneous interac-

tion of both the duplex and the quadruplex region with the same thrombin molecule, and the binding does not involve the duplex, but only the quadruplex domain, as observed for TBA-like aptamers (29–31). This behaviour is markedly different from that of HD22, the other duplex/quadruplex thrombin-binding aptamer, whose structure has been elucidated by X-ray crystallography (33). In HD22 aptamer, the first guanine of the quadruplex is directly linked to the last residue of the duplex and the transition is mediated by a G-fork between the first guanine of the quadruplex and a linker residue. This kind of junction determines the formation of a distorted G-quadruplex structure and an almost orthogonal orientation of the helical axes of the two motifs. In this bend conformation both the duplex and the quadruplex can interact with exosite II of thrombin, which has a significantly larger surface than exosite I, the binding site of RE31 and TBA-like nucleotides.

In the present crystal, the duplex of RE31 establishes contacts with three different regions of the protein surface of symmetry related thrombin molecules. Although these contacts involve a smaller number of interactions with respect to the aptamer/protein binding site described above, they may contribute to the greater protein affinity measured for RE31 with respect to TBA (27). On the other hand, the compact structure of the aptamer, and in particular the recruitment of the TGT loop in the junction, may increase the resistance to nucleases that primarily attack single-stranded oligonucleotide fragments (quadruplex loops) (45,46) and explain the greater inhibitory effect of RE31 compared to that provided by TBA. Furthermore, it can be surmised that the presence of the duplex phosphodiester bonds, whose rupture is not likely to affect the functionality of the aptamer, may also contribute to a decrease of the nuclease efficiency.

As a final comment, it is worth to stress that RE31 and HD22, which have the duplex motif at the 5′ and 3′ ends of a quadruplex core, exemplify a different structural case with respect to the constructs designed and characterized by Phan and co-workers (17,18,47,48). In the latter case, the duplex region is inserted in a loop of well-structured G-quadruplexes, where it produces negligible effects on the quadruplex architecture. The RE31 model shows that the link of an antiparallel B-form duplex to an antiparallel G-quadruplex may occur with an almost gradual transition from one structural motif to the other, allowing the regularity of both domains to be preserved through the formation of a continuous base stacking. On the other hand, for HD22 the preservation of the duplex structural features, severely affects the regularity of the quadruplex (33).

In conclusion, the present thrombin-RE31 structure represents the first atomic resolution model of a hybrid duplex–quadruplex aptamer interacting with protein exosite I. This structure, in comparison with the different architecture of HD22, proves that structural characterization of duplex/quadruplex and quadruplex/duplex molecules is a fascinating topic worth to be deeply analysed. Indeed the sterically accessible space for residues that connect the two motifs allows varied and unpredictable conformations of the link and appears to play an important role in determining functional properties of these oligonucleotides.

## ACCESSION NUMBER

PDB code: 5CMX.

## SUPPLEMENTARY DATA

Supplementary Data are available at NAR Online.

## ACKNOWLEDGEMENTS

We acknowledge Giosuè Sorrentino and Maurizio Amendola (Institute of Biostructures and Bioimages, Naples, Italy) for technical assistance.

## FUNDING

RFBR (Russian Foundation of Basic Research) [N 16-04-00484]. Funding for open access charge: RFBR [N 16-04-00484].
*Conflict of interest statement*. None declared.

## REFERENCES

1. Ghosh,A. and Bansal,M. (2003) A glossary of DNA structures from A to Z. *Acta Crystallogr. D Biol. Crystallogr.*, **59**, 620–626.
2. Leslie,A.G., Arnott,S., Chandrasekaran,R. and Ratliff,R.L. (1980) Polymorphism of DNA double helices. *J. Mol. Biol.*, **143**, 49–72.
3. Duca,M., Vekhoff,P., Oussedik,K., Halby,L. and Arimondo,P.B. (2008) The triple helix: 50 years later, the outcome. *Nucleic Acids Res.*, **36**, 5123–5138.
4. Lilley,D.M. and Clegg,R.M. (1993) The structure of the four-way junction in DNA. *Annu. Rev. Biophys. Biomol. Struct.*, **22**, 299–328.
5. Gueron,M. and Leroy,J.L. (2000) The i-motif in nucleic acids. *Curr. Opin. Struct. Biol.*, **10**, 326–331.
6. Burge,S., Parkinson,G.N., Hazel,P., Todd,A.K. and Neidle,S. (2006) Quadruplex DNA: sequence, topology and structure. *Nucleic Acids Res.*, **34**, 5402–5415.
7. Neidle,S. (2010) Human telomeric G-quadruplex: the current status of telomeric G-quadruplexes as therapeutic targets in human cancer. *FEBS J.*, **277**, 1118–1125.
8. Bidzinska,J., Cimino-Reale,G., Zaffaroni,N. and Folini,M. (2013) G-quadruplex structures in the human genome as novel therapeutic targets. *Molecules*, **18**, 12368–12395.
9. Qin,Y. and Hurley,L.H. (2008) Structures, folding patterns, and functions of intramolecular DNA G-quadruplexes found in eukaryotic promoter regions. *Biochimie*, **90**, 1149–1171.
10. Campbell,N., Collie,G.W. and Neidle,S. (2012) Crystallography of DNA and RNA G-quadruplex nucleic acids and their ligand complexes. *Curr. Protoc. Nucleic Acid Chem.*, Chapter 17, Unit 17.16.
11. Adrian,M., Heddi,B. and Phan,A.T. (2012) NMR spectroscopy of G-quadruplexes. *Methods*, **57**, 11–24.
12. Mergny,J.L. (2013) Meeting Report: Fourth international meeting on G-quadruplex Nucleic Acids (Singapore, July 1–4, 2013). *Biochimie*, **95**, 2320–2325.
13. Xu,Y. (2011) Chemistry in human telomere biology: structure, function and targeting of telomere DNA/RNA. *Chem. Soc. Rev.*, **40**, 2719–2740.
14. Xu,Y., Ishizuka,T., Kurabayashi,K. and Komiyama,M. (2009) Consecutive formation of G-quadruplexes in human telomeric-overhang DNA: a protective capping structure for telomere ends. *Angew. Chem.*, **48**, 7833–7836.
15. Russo Krauss,I., Parkinson,G.N., Merlino,A., Mattia,C.A., Randazzo,A., Novellino,E., Mazzarella,L. and Sica,F. (2014) A regular thymine tetrad and a peculiar supramolecular assembly in the first crystal structure of an all-LNA G-quadruplex. *Acta Crystallogr. D Biol. Crystallogr.*, **70**, 362–370.
16. Ren,J., Qu,X., Trent,J.O. and Chaires,J.B. (2002) Tiny telomere DNA. *Nucleic Acids Res.*, **30**, 2307–2315.
17. Lim,K.W. and Phan,A.T. (2013) Structural basis of DNA quadruplex-duplex junction formation. *Angew. Chem.*, **52**, 8566–8569.

18. Lim,K.W., Khong,Z.J. and Phan,A.T. (2014) Thermal stability of DNA quadruplex-duplex hybrids. *Biochemistry*, **53**, 247–257.
19. Bock,L.C., Griffin,L.C., Latham,J.A., Vermaas,E.H. and Toole,J.J. (1992) Selection of single-stranded DNA molecules that bind and inhibit human thrombin. *Nature*, **355**, 564–566.
20. Burke,J.M. and Berzal-Herranz,A. (1993) In vitro selection and evolution of RNA: applications for catalytic RNA, molecular recognition, and drug discovery. *FASEB J.*, **7**, 106–112.
21. Mayer,G. (2009) The chemical biology of aptamers. *Angew. Chem.*, **48**, 2672–2689.
22. Ulrich,H. (2005) DNA and RNA aptamers as modulators of protein function. *Med. Chem.*, **1**, 199–208.
23. Gatto,B., Palumbo,M. and Sissi,C. (2009) Nucleic acid aptamers based on the G-quadruplex structure: therapeutic and diagnostic potential. *Curr. Med. Chem.*, **16**, 1248–1265.
24. Tasset,D.M., Kubik,M.F. and Steiner,W. (1997) Oligonucleotide inhibitors of human thrombin that bind distinct epitopes. *J. Mol. Biol*, **272**, 688–698.
25. Ikebukuro,K., Okumura,Y., Sumikura,K. and Karube,I. (2005) A novel method of screening thrombin-inhibiting DNA aptamers using an evolution-mimicking algorithm. *Nucleic Acids Res.*, **33**, e108.
26. Mazurov,A.V., Titaeva,E.V., Khaspekova,S.G., Storojilova,A.N., Spiridonova,V.A., Kopylov,A.M. and Dobrovolsky,A.B. (2011) Characteristics of a new DNA aptamer, direct inhibitor of thrombin. *Bull. Exp. Biol. Med.*, **150**, 422–425.
27. Spiridonova,V.A., Barinova,K.V., Glinkina,K.A., Melnichuk,A.V., Gainutdynov,A.A., Safenkova,I.V. and Dzantiev,B.B. (2015) A family of DNA aptamers with varied duplex region length that forms complexes with thrombin and prothrombin. *FEBS Lett.*, **589**, 2043–2049.
28. Spiridonova,V.A., Glinkina,K.A., Gainutdinov,A.A. and Arutyunyan,A.M. (2014) Production of thrombin complexes with DNA aptamers containing G-quadruplex and different duplexes. *J. Nephrol. Ther.*, **4**, 149–154.
29. Russo Krauss,I., Merlino,A., Giancola,C., Randazzo,A., Mazzarella,L. and Sica,F. (2011) Thrombin-aptamer recognition: a revealed ambiguity. *Nucleic Acids Res.*, **39**, 7858–7867.
30. Russo Krauss,I., Merlino,A., Randazzo,A., Novellino,E., Mazzarella,L. and Sica,F. (2012) High-resolution structures of two complexes between thrombin and thrombin-binding aptamer shed light on the role of cations in the aptamer inhibitory activity. *Nucleic Acids Res.*, **40**, 8119–8128.
31. Pica,A., Russo Krauss,I., Merlino,A., Nagatoishi,S., Sugimoto,N. and Sica,F. (2013) Dissecting the contribution of thrombin exosite I in the recognition of thrombin binding aptamer. *FEBS J.*, **280**, 6581–6588.
32. Dolinnaya,N.G., Yuminova,A.V., Spiridonova,V.A., Arutyunyan,A.M. and Kopylov,A.M. (2012) Coexistence of G-quadruplex and duplex domains within the secondary structure of 31-mer DNA thrombin-binding aptamer. *J. Biomol. Struct. Dyn.*, **30**, 524–531.
33. Russo Krauss,I., Pica,A., Merlino,A., Mazzarella,L. and Sica,F. (2013) Duplex-quadruplex motifs in a peculiar structural organization cooperatively contribute to thrombin binding of a DNA aptamer. *Acta Crystallogr. D Biol. Crystallogr.*, **69**, 2403–2411.
34. Russo Krauss,I., Merlino,A., Randazzo,A., Mazzarella,L. and Sica,F. (2010) Crystallization and preliminary X-ray analysis of the complex of human alpha-thrombin with a modified thrombin-binding aptamer. *Acta Crystallogr. F Struct. Biol. Cryst. Commun.*, **66**, 961–963.
35. Otwinowski,Z. and Minor,W. (1997) Processing of X-ray diffraction data collected in oscillation mode. *Method Enzymol.*, **276**, 307–326.
36. McCoy,A.J., Grosse-Kunstleve,R.W., Storoni,L.C. and Read,R.J. (2005) Likelihood-enhanced fast translation functions. *Acta Crystallogr. D Biol. Crystallogr.*, **61**, 458–464.
37. Murshudov,G.N., Skubak,P., Lebedev,A.A., Pannu,N.S., Steiner,R.A., Nicholls,R.A., Winn,M.D., Long,F. and Vagin,A.A. (2011) REFMAC5 for the refinement of macromolecular crystal structures. *Acta Crystallogr. D Biol. Crystallogr.*, **67**, 355–367.
38. Adams,P.D., Afonine,P.V., Bunkoczi,G., Chen,V.B., Davis,I.W., Echols,N., Headd,J.J., Hung,L.W., Kapral,G.J., Grosse-Kunstleve,R.W. *et al.* (2010) PHENIX: a comprehensive Python-based system for macromolecular structure solution. *Acta Crystallogr. D Biol. Crystallogr.*, **66**, 213–221.
39. Emsley,P. and Cowtan,K. (2004) Coot: model-building tools for molecular graphics. *Acta Crystallogr. D Biol. Crystallogr.*, **60**, 2126–2132.
40. Pettersen,E.F., Goddard,T.D., Huang,C.C., Couch,G.S., Greenblatt,D.M., Meng,E.C. and Ferrin,T.E. (2004) UCSF chimera - A visualization system for exploratory research and analysis. *J. Comput. Chem.*, **25**, 1605–1612.
41. Lu,X.J. and Olson,W.K. (2008) 3DNA: a versatile, integrated software system for the analysis, rebuilding and visualization of three-dimensional nucleic-acid structures. *Nat. Protoc.*, **3**, 1213–1227.
42. Krissinel,E. and Henrick,K. (2004) Secondary-structure matching (SSM), a new tool for fast protein structure alignment in three dimensions. *Acta Crystallogr. D Biol. Crystallogr.*, **60**, 2256–2268.
43. Vangone,A., Spinelli,R., Scarano,V., Cavallo,L. and Oliva,R. (2011) COCOMAPS: a web application to analyze and visualize contacts at the interface of biomolecular complexes. *Bioinformatics*, **27**, 2915–2916.
44. Mihel,J., Sikic,M., Tomic,S., Jeren,B. and Vlahovicek,K. (2008) PSAIA - protein structure and interaction analyzer. *BMC Struct. Biol.*, **8**, 21.
45. Bishop,J.S., Guy-Caffey,J.K., Ojwang,J.O., Smith,S.R., Hogan,M.E., Cossum,P.A., Rando,R.F. and Chaudhary,N. (1996) Intramolecular G-quartet motifs confer nuclease resistance to a potent anti-HIV oligonucleotide. *J. Biol. Chem.*, **271**, 5698–5703.
46. Zhang,N., Bing,T., Xiangjun,L., Qi,C., Shen,L., Wang,L. and Shangguan,D. (2015) Cytotoxicity of guanine-based degradation products contributes to the antiproliferative activity of guanine-rich oligonucleotides. *Chem. Sci.*, **6**, 3831–3838.
47. Lim,K.W., Nguyen,T.Q. and Phan,A.T. (2014) Joining of multiple duplex stems at a single quadruplex loop. *J. Am. Chem. Soc.*, **136**, 17969–17973.
48. Lim,K.W., Jenjaroenpun,P., Low,Z.J., Khong,Z.J., Ng,Y.S., Kuznetsov,V.A. and Phan,A.T. (2015) Duplex stem-loop-containing quadruplex motifs in the human genome: a combined genomic and structural study. *Nucleic Acids Res.*, **43**, 5630–5646.